*Estuarine, Coastal and Shelf Science* (2000) **50,** 315–331
doi:10.1006/ecss.2000.0548, available online at http://www.idealibrary.com on IDEAL®

# Flow and Sediment Transport on a Tidal Salt Marsh Surface

**T. Christiansen[a], P. L. Wiberg[a] and T. G. Milligan[b]**

[a]*University of Virginia, Department of Environmental Sciences, Clark Hall, Charlottesville, Virginia 22903, U.S.A.*
[b]*Fisheries and Oceans Canada, Bedford Institute of Oceanography, Marine Environmental Sciences Division, P.O. Box 1006, Dartmouth NS B2Y 4A2, Canada*

*Received 19 November 1998 and accepted in revised form 22 July 1999*

The physical processes that control mineral sediment deposition on a mesotidal salt marsh surface on the Atlantic Coast of Virginia were characterized through a series of measurements of sediment concentration, flow velocity, turbulence, water surface elevation, marsh topography and particle size distributions of sediment deposited on the marsh surface. The comprehensive nature of the data set allowed assessment of the temporal and spatial variability in marsh surface deposition, the variability in depositional processes among tides of different amplitudes, as well as the specific processes that control deposition on this tidal marsh. Through three different types of measurements, it was found that sediment deposition occurred on the marsh surface during rising tides at tidal elevations ranging from those barely flooding the creek bank to high spring tides, and that sediment was not remobilized by tidal flows after initial deposition. Sediment deposition occurred on this marsh surface largely because fine sediment in suspension formed flocs. Analysis of inorganic grain size distributions of sediment deposited within 8 m of the tidal creek indicated that 70–80% of this sediment was deposited in a flocculated form. The rest (particles larger than 20 μm) were deposited as individual particles. In the marsh interior, 25 m from the tidal creek, single grain settling predominated. Reduction of turbulence levels within the vegetation canopy on the marsh also promoted particle settling. The processes controlling sediment deposition did not vary among tides. However, suspended sediment concentrations near the creek bank increased with increasing tidal amplitude, consequently promoting higher rates of deposition on higher tides. 

**Keywords:** mineral sediment deposition; salt marsh; sediment and flow dynamics; process variability; tidal variability; grain size distributions; U.S. Atlantic Coast; Virginia Coast Reserve Long Term Ecological Research

## Introduction

Coastal salt marshes are located at the boundary between ocean and land. The organisms in this environment have adapted to intertidal conditions, but it has been shown that the ecological stability of these systems is sensitive to the marsh surface elevation relative to mean sea-level (Stevenson *et al.*, 1985). Relative sea-level rise, organic matter accumulation and mineral sediment input affect the vertical position of the marsh surface (Cahoon *et al.*, 1995). Consequently, long term assessment of the fate of marshes that maintain their elevation by accumulating mineral sediment depends on accurate understanding of the physical processes that control mineral sediment deposition on the marsh surface.

Earlier studies have addressed several aspects of mineral sediment deposition on marshes. For example, mineral accumulation of sediment occurs during times when the vegetated marsh surface is flooded and suspended sediment moves with the flow onto the marsh surface (Wang *et al.*, 1993; Leonard *et al.*, 1995). Sediment deposition on marsh surfaces is spatially variable (French *et al.*, 1995; Leonard, 1997) with more sediment depositing in proximity to the tidal creek, the primary sediment source. The distance a particle travels before settling out of suspension is determined by the horizontal flow velocity (Burke & Stoltzenbach, 1983; Leonard & Luther, 1995; Wang *et al.*, 1993), turbulent energy of the flow (Leonard & Luther, 1995; Kadlec, 1990; Tsujimoto *et al.*, 1991) and particle settling velocity (Sternberg *et al.*, 1999). Flow across a marsh is strongly affected by marsh vegetation. Spectra of the turbulence structure within a *Spartina alterniflora* canopy indicate that the turbulence structure is modified by breaking down larger turbulent eddies that transfer the majority of momentum in the flow (Leonard & Luther, 1995).

Despite this progress in the understanding of depositional processes on marshes, a number of important questions remain. Earlier studies only measured up to four different tidal cycles. Consequently, the variability in depositional process among tides of different amplitudes could not be determined. Particle settling

0272–7714/00/030315+17 $35.00/0 

rates, and particularly the significance of flocculation in promoting deposition on salt marshes, need to be investigated. The effect of vegetation on flow over marsh surfaces, combined with the cohesive nature of marsh surface sediments, has made it difficult to determine whether shear stresses acting within the vegetation canopy are capable of remobilizing marsh sediment after initial deposition. The potential for remobilization and redistribution of marsh sediment after initial deposition has to be known before net rates and patterns of deposition on tidal salt marshes can be established.

Phillips Creek marsh, a mesotidal, mainland fringing marsh on the Atlantic coast of Virginia (U.S.A.), is an example of a marsh that increases its vertical elevation primarily by accumulating mineral sediment on the marsh surface (Kastler & Wiberg, 1996). In this study, the depositional processes on the surface of Phillips Creek marsh were characterized using high resolution measurements of sediment concentration, flow velocity, turbulence, water surface elevation, marsh surface topography and particle size distributions of sediment deposited on the marsh surface. In particular, the goal was to determine specific sediment transport patterns and shear stresses acting on the marsh surface as a function of time and of distance from the tidal creek. The measurements were made at the widest possible range of tidal conditions, from tides barely flooding the marsh surface to infrequent storm surges. An additional objective was to determine whether turbulence reduction within the vegetation canopy and flocculation of fine grained suspended sediment were important processes promoting sediment deposition on Phillips Creek marsh.

## Study site

The marsh selected for this study is a mainland fringing marsh located in the Phillips Creek area of Hog Island Bay on the Atlantic side of the Delmarva Peninsula (Figure 1). On the Eastern Shore of Virginia, along the Atlantic side of the Delmarva Peninsula, a 100 km long chain of barrier islands protects the bay waters between the peninsula mainland and the barrier islands. The bay between the mainland and barrier islands consists of shoals and marshes dissected by a few very deep channels that provide an efficient exchange of water in the bay (Figure 1). The tidal range on the mainland is similar to the tidal range in the ocean: 1·5–2 m. The marshes in the bay and the fringing low marshes are entirely vegetated with *S. alterniflora*, whereas the shoals are unvegetated. The surface of Phillips Creek low marsh is fully inundated on the highest part of the highest tides, but the vegetation typically protrudes through the water surface.

The mean organic content of the marsh sediment in Phillips Creek low marsh is 6·5% (Kastler, 1993). The marsh surface sediments in the Phillips Creek area are primarily in the silt and clay size range ($D$<62·5 μm). Particles coarser than 62·5 μm are typically marsh fiddler crab (*Uca* sp.) fecal material. The silt sized sediments are primarily quartz, whereas the clay mineralogy is dominated by illite (Kastler, 1993; Robinson, 1994). Robinson (1994) also found that sediments from the mainland tidal creeks have similar clay mineralogy to sediments found on the marsh surface and to suspended sediment, indicating that the tidal channels are the source of sediment deposited on the marsh surface.

The area around Chesapeake Bay is responding to subsidence related to post glacial effects (Nerem *et al.*, 1998). Calculated subsidence rates on the Delmarva Peninsula were 1·1 to 1·2 mm year$^{-1}$ (Peltier & Jiang, 1996). Estimates of mean relative sea-level rise (eustatic sea-level rise plus subsidence) in Chesapeake Bay include rates of 2 mm year$^{-1}$ (Holdahl & Morrison, 1974), 3·1 mm year$^{-1}$ (Emery & Aubrey, 1991) and 3·5 mm year$^{-1}$ (Nerem *et al.*, 1998). Phillips Creek marsh is currently expanding landwards (encroaching on upland) in response to sea-level rise (Kastler & Wiberg, 1996). Long term sediment deposition rates determined by $^{210}$Pb dating of sediment cores suggest that Phillips Creek marsh is accreting at a rate of 0·9–1·4 mm per year (Kastler & Wiberg, 1996).

## Methods

### *Experimental setup*

At the study site in Phillips Creek marsh, a transect with five stations was set up perpendicular to the adjacent tidal creek (Figure 1). The transect extended 50 m from the bank of the tidal creek to the marsh interior. Three stations were established within close proximity of one another on the creek bank because the largest gradients in sediment deposition were expected in this area. The remaining two stations were set up in the marsh interior, away from the creek bank. At each station, time series of turbidity and of flow speed and direction during inundation events were measured. The topography of the marsh surface was surveyed at high resolution, with a surveyed point approximately every 2 m$^2$. Water level was monitored on the marsh surface and at a nearby tide gauge in Redbank, Virginia. The tidal elevations measured at

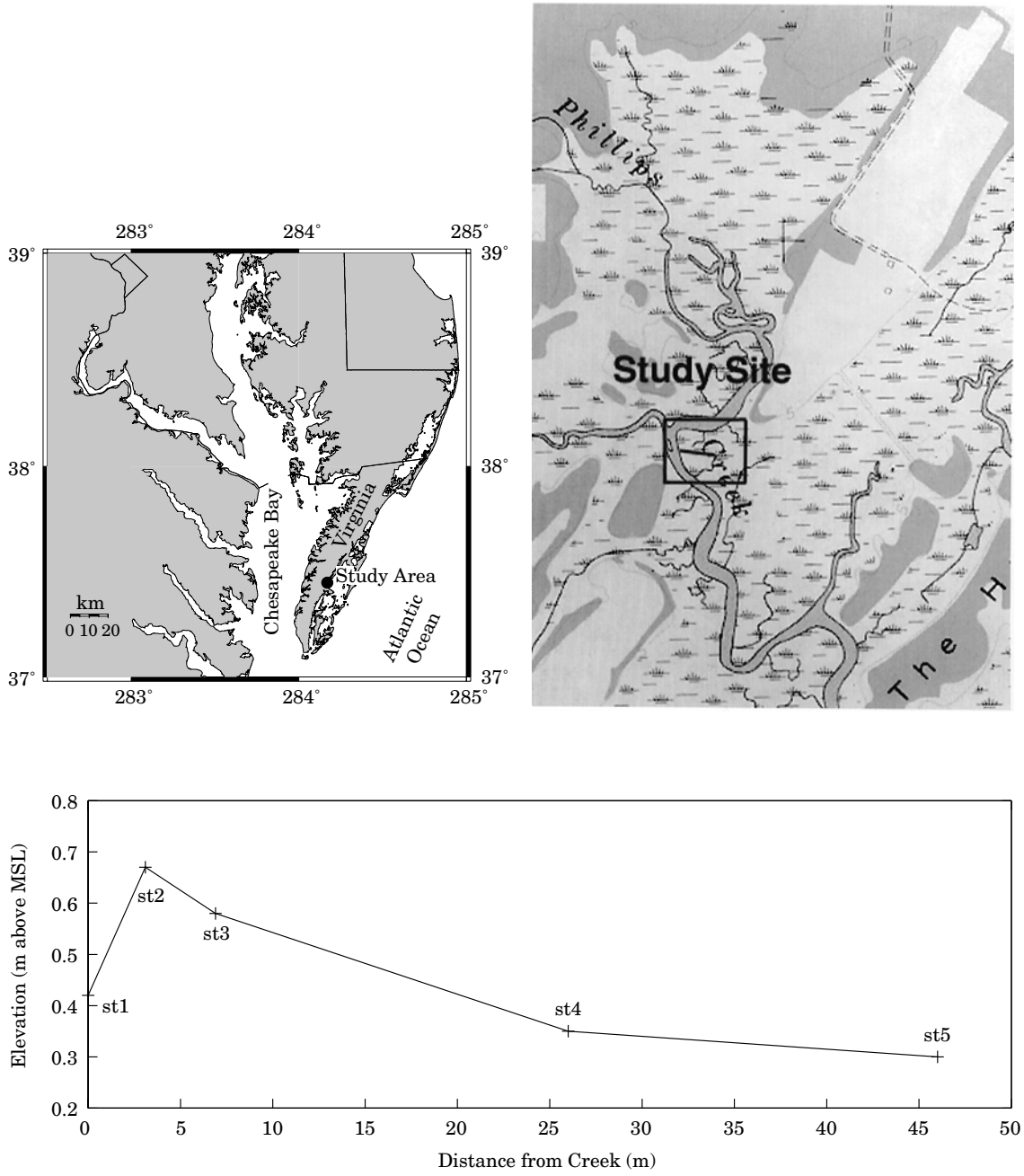


FIGURE 1. (a) Location of study site on the Delmarva Peninsula. (b) Location of transect in Phillips Creek marsh. (c) Elevation and relative location of sampling stations along transect.

that tide gauge were related to the elevation of the marsh surface by adjusting the tide gauge readings to the same datum as the marsh surface topography. A year-long record of measured tides (591 tidal cycles) from the Redbank tide gauge was used to determine inundation frequency across the marsh (Figure 2). The marsh surface was fully inundated on 40% of tidal cycles when the highest points on the levees (80 cm above mean sea level) were flooded.

*Velocity measurements*

Velocity measurements were made using a SonTek Acoustic Doppler Velocimeter (ADV) to measure high frequency velocity variations and mean flow velocity in two horizontal directions and in the vertical. The ADV was programmed to sample at 10 Hz, in 15 or 20 min bursts for 5 h during each tidal cycle. The instrument was positioned 10 cm above the bottom so that measurements could be made during

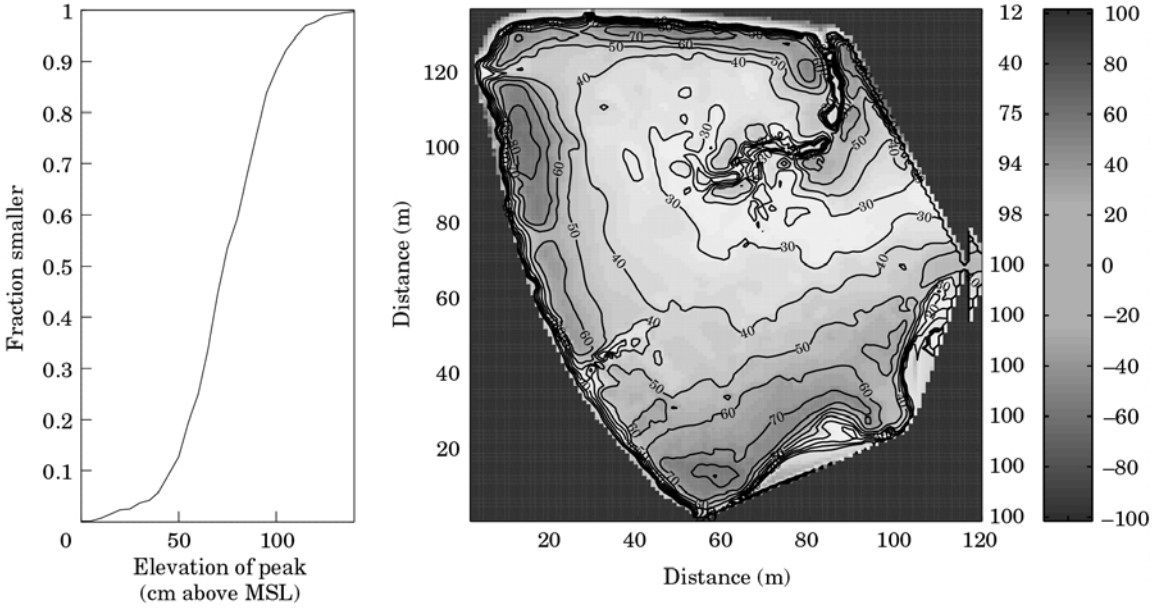


FIGURE 2. Inundation frequencies of the marsh surface. The left panel shows the distribution of tidal amplitudes for 591 tidal cycles measured in 1994 at Redbank tide gauge, approximately 1 km from the study site. The right panel shows a contour plot of the marsh surface with contour levels in cm above mean sea level. The bar to the right of the contour plot is labelled with contour levels on the right and inundation frequency in percent of tidal cycles on the left.

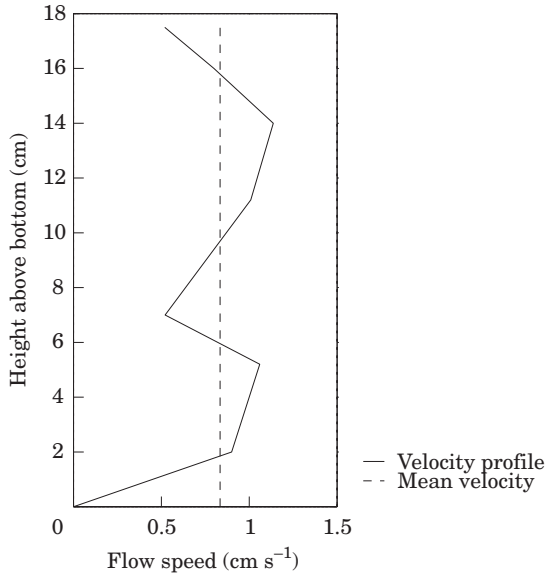


FIGURE 3. Velocity profile and mean velocity. The profile was measured at a lower location (where the levee is breached at coordinates (40,40) on Figure 2) at the study site approximately 20 m south of the transect, on a rising tide with an amplitude of 85 cm.

the majority of the tidal flooding period and to measure at an elevation corresponding approximately to the elevation of mean flow velocity (Figure 3). After the instrument was set up, its orientation was determined using a compass, and vertical orientation was ensured with a level. The current meter was always oriented with the positive x-direction towards west.

*Turbulence characteristics*

High frequency velocity measurements were used to calculate Reynolds stresses for flow on the marsh. Each velocity time series was divided into segments of 2048 data points (equivalent to 3·4 min segments). The flow could be considered steady within this time period, and the mean flow velocity in each of the three dimensions was calculated as the mean of the 2048 measurements. The magnitude of the high frequency velocity fluctuations was determined by subtracting the mean from the measured velocity. These were used to calculate the turbulent kinetic energy, $q=\frac{1}{2}\sqrt{\overline{u'^2+v'^2+w'^2}}$ and the horizontal components of shear stress, $\tau_{zx}=-\rho\overline{w'u'}$ and $\tau_{zy}=-\rho\overline{w'v'}$. The horizontal shear stresses are the stresses responsible for vertical transfer of momentum in the flow (Tennekes & Lumley, 1972), and at the bottom, these stresses, if they are sufficiently large, are responsible for entraining sediment into the flow. The two horizontal stresses were combined to calculate $\tau=\sqrt{\tau_{zx}^2+\tau_{zy}^2}$, the mean stress 10 cm above the bed (the level of velocity measurements).

The effectiveness of turbulence in maintaining sediment in suspension was evaluated using the

Rouse number: $P_m = w_s/u_\star$, where $w_s$ is particle settling velocity, $u_\star = \sqrt{\frac{\tau_b}{\rho}}$ is the shear velocity and $\tau_b$ is the stress at the bed. When $P_m > 1$, sediment cannot be maintained in suspension, and when $P_m < 0{\cdot}3$, sediment is maintained in suspension. Because $w_s$ depends on grain size and $u_\star$ changes with flow conditions, the Rouse number is a function of these parameters as well. The vertical profile of shear stress within a vegetation canopy tends to be more uniform than that of an unobstructed shear flow (e.g. Tsujimoto *et al.*, 1991). As a result, the shear stress measured 10 cm above the boundary, $\tau$, provides a reasonable approximation to the shear stress acting on the boundary, $\tau_b$. The shear velocity obtained from this estimate of boundary shear stress was used with the Rouse number thresholds for suspension to evaluate the limits on settling velocity of particles in suspension.

### *Turbidity measurements*

Time series of suspended sediment concentration were measured at a range of concentrations and water levels. The measurements were made using SEA-TECH optical back scatter (OBS) sensors. The OBS sensors measure turbidity by emitting an infrared light and measuring the backscatter of this light. The back-scattered signal must be calibrated to obtain sediment concentration. Sensor response is sensitive to grain size (Wiberg *et al.*, 1994), and was calibrated in a laboratory facility using sediment found at Phillips Creek marsh. The calibrated relationship between the OBS signal and concentration of particles in the water was linear, with an $R^2 = 0{\cdot}999$. The three sensors used in this study had very similar response which made comparison of measurements reliable. The OBS sampling frequency was adjustable, and frequencies of one measurement every 2 or 3 s were used.

### *Particle size analysis*

Particle size analysis was performed on the fully disaggregated inorganic mineral fraction of a subsample of the unconsolidated bed sediment deposited on sediment traps positioned at stations 1, 2, 3 and 4, over a two week period. The size analysis was performed with a Coulter Multisizer IIe using the methods described in Milligan and Kranck (1991) and provided the frequency distribution of the grain sizes present in the sample.

A disaggregated grain size distribution can be decomposed into two or three components: sediment that settled as flocs, sediment that settled as single grains, and, if present, sediment that has been remobilized after initial deposition (Kranck *et al.*, 1996*a*; Milligan & Loring, 1997). The relative frequency of each grain size (also referred to as concentration, $C$) is plotted as a function of particle diameter on a log–log scale. The distribution is described by the relationship between concentration $C$ and diameter:

$$\log C = \log(\Delta Q) + (m+n)\left(\log\left(\frac{(\rho_s - \rho_f)g}{18\mu}\right) + 2\log D\right) - \bar{k}\frac{(\rho_s - \rho_f)gD^2}{18\mu} \quad (1)$$

where $log\ (\Delta Q)$ and $\bar{k}$ are regression coefficients derived from fitting Equation 1 to the measured grain size distributions. The value of $m$ for the floc portion of the curve (fine-grained limb), called the source slope, has a value close to 0, and is determined by the nature of the source for the material in suspension (Kranck *et al.*, 1996*a*). For this study, $m$, determined by fitting a straight line to the floc tail, has a value of 0·2. The coefficient $n$ describes the mode of deposition; it has a value of 0 for deposition from a flocculated source and a value of 1 for single grain deposition (Milligan & Loring, 1997; Kranck *et al.*, 1996*a*,b).

Curves representing the floc and single-grain portions of the measured size distributions were obtained by fitting Equation 1 to the fine (with $n = 0$) and the coarse (with $n = 1$) ends of the distributions (Kranck *et al.*, 1996*a*). The grain size at which these two curves intersect, termed the floc limit, is an indication of the upper limit on the size of particles incorporated into flocs and the lower limit on the size of particles present as individual grains in suspension (Milligan & Loring, 1997). When the two curves are superimposed, they approximate the original particle size distribution.

### *Particle settling rates*

Settling rate of small individual particles is often calculated using Stokes law:

$$w_s = \frac{(\rho_s - \rho_f)gD^2}{18\mu} \quad (2)$$

where $\rho_s$ is particle density, $\rho_f$ is fluid density, $g$ is gravitational acceleration, $D$ is particle size, and μ is fluid viscosity. Silt and clay sized sediments are frequently deposited in a flocculated form. Flocs have a lower settling velocity (due to lower density) than individual particles of the same size, but a higher settling velocity than individual constituent particles. Sternberg *et al.* (1999) used the settling velocity

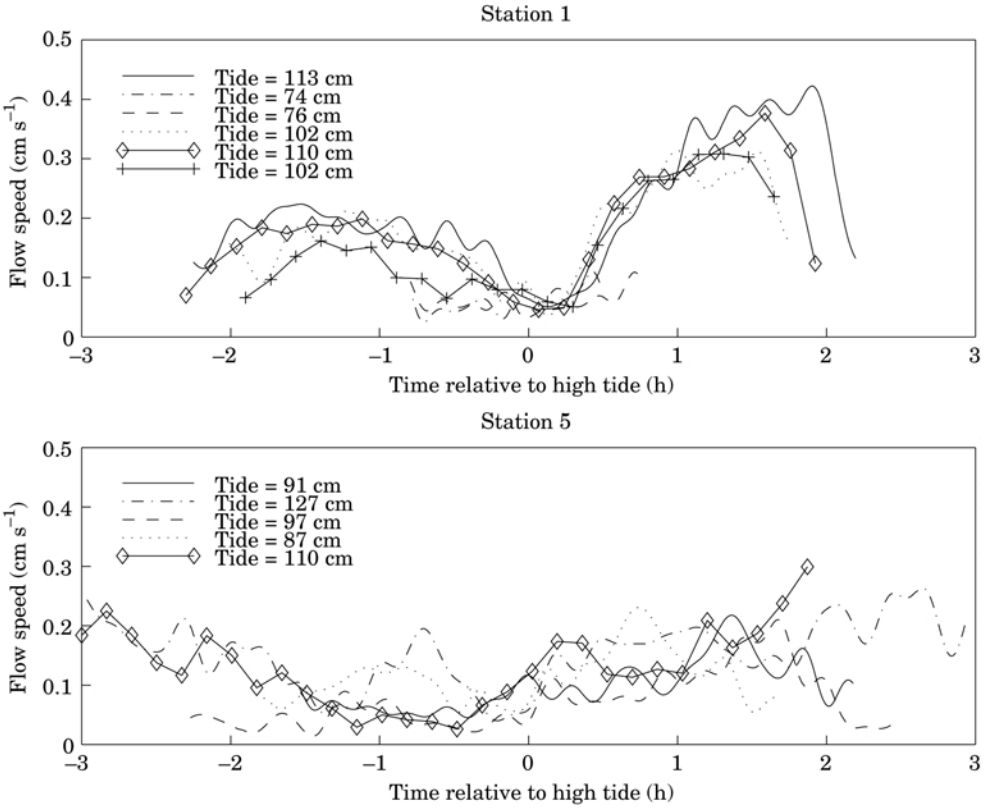


FIGURE 4. Comparison of measured flow speeds at a range of tidal amplitudes at stations 1 and 5.

measured with an *in situ* video camera in conjunction with the measurements of particle size to derive a relationship between settling velocity $w_s$ and floc diameter $D$ for flocs on the northern California continental shelf:

$$w_s = 0{\cdot}0002 D_{\mu m}^{1{\cdot}54} \quad (3)$$

The particle diameter is measured in μm and the unit of settling velocity is mm s$^{-1}$.

## Measurements and results

### *Velocity measurements*

Flow conditions on the marsh surface were measured throughout the duration of tidal flooding at stations along the sampling transect during 35 different tidal cycles, with tidal amplitudes ranging from 80–135 cm above mean sea level (MSL). Tidal elevations of 80 cm or higher, which fully inundated the marsh surface, occurred on 40% of tidal cycles. A tidal amplitude of 135 cm above MSL occurred on average once every two months (Figure 2).

There is little variation in flow velocity on the marsh among stations and among tides of different amplitudes relative to flow velocity in the tidal creek. Velocities measured on the creek bank (station 1) were higher and showed a more pronounced separation between rising and falling tide than velocities measured at station 5 in the marsh interior (Figure 4). Flow velocities at all locations along the transect were extremely low. The highest velocities were measured at the onset and at the end of a flooding period, but even the highest velocities were less than 1 cm s$^{-1}$, more than one order of magnitude lower than flow velocities in the tidal creek. Velocities were slightly higher during falling tides than during rising tides, suggesting a slight ebb dominated tidal asymmetry. The period of flooding varied depending on tidal amplitude and location on the marsh surface. Station 5 was located at a lower elevation than station 1, and was consequently flooded for a larger part of a tidal cycle than station 1. For example, during a tide with an amplitude of 110 cm, station 1 was flooded for approximately 4 h whereas station 5 was flooded for more than 5 h. The flow direction changed throughout the duration of tidal flooding. The predominant

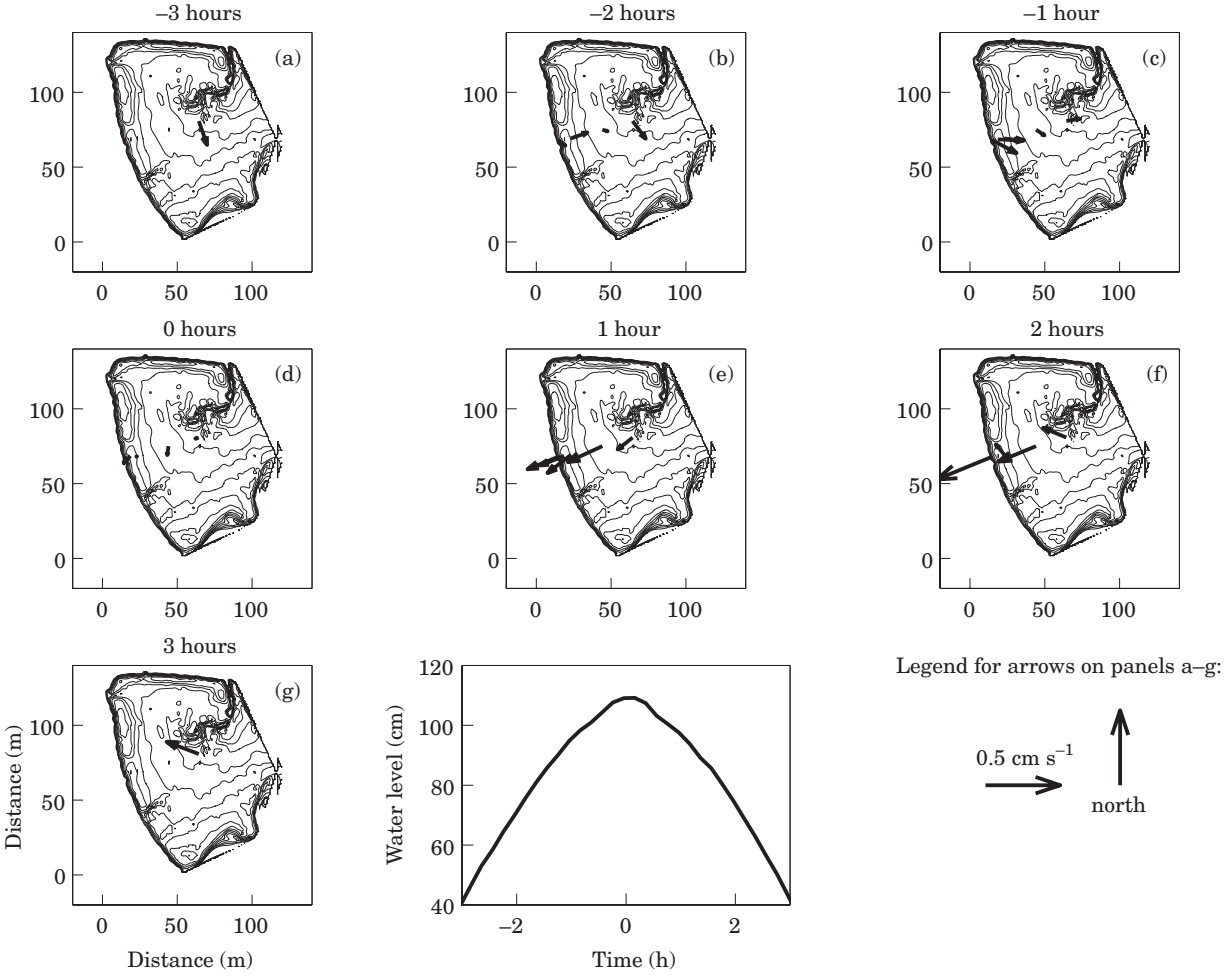


FIGURE 5. Circulation on marsh surface. Each panel represents a 1 h time step throughout a 6 h period of marsh surface flooding. Flow vectors represent velocity and flow direction at each station, and at each time step. Panel (h) represents water level variation during the inundation period. This flow pattern was typical for tides that fully inundated the marsh surface.

flow direction on the rising tide was from Phillips Creek towards the marsh interior, on the falling tide the flow direction was reversed (Figure 5).

### *The effect of marsh vegetation on the flow*

Marsh surface vegetation provided an important control on flow within the vegetation canopy by modifying both mean velocity and the turbulent properties of the flow. Velocity measurements were made over a period of 8 months, with emphasis on winter months because water levels were higher during this time. Vegetation densities, however, were not constant in this period. Vegetation densities along the transect are described in terms of an upper and a lower limit, in terms of an estimated stem diameter and in terms of plant height (Table 1). The plants on the creek bank were thicker and taller, but less dense, than plants in the interior. The magnitude of the effect of the vegetation on the flow was assessed by comparing conditions both within the canopy and in the tidal creek immediately adjacent (upstream on the rising tide, downstream on the falling tide) to the vegetation boundary.

In the tidal creek, the turbulent energy spectrum (Figure 6) had the characteristics of a fully developed turbulent flow with a slope of $-5/3$ in the inertial subrange (Tennekes & Lumley, 1972). At station 1, which was located within the vegetation canopy, 2 m from where the creek measurements were made, the energy at the lower frequency was reduced relative to the flow in the tidal creek. As the flow propagated further into the canopy, the energy in the low frequency end of the spectra was further reduced. The reduction in energy at low frequencies suggests that the vegetation inhibits production

TABLE 1. Vegetation densities and stem thickness at each sampling location

| | Station 1 | Station 2 | Station 3 | Station 4 | Station 5 |
|---|---|---|---|---|---|
| Stem density (stems $m^{-2}$) | 124–172 | 148–204 | 136–188 | 88–212 | 92–148 |
| Stem diameter (cm) | 0·9–1·1 | 0·6–1 | 0·6–0·8 | 0·5–0·7 | 0·6–0·8 |
| Plant height (cm) | 85–110 | 65–75 | 45–85 | 50–65 | 65–86 |

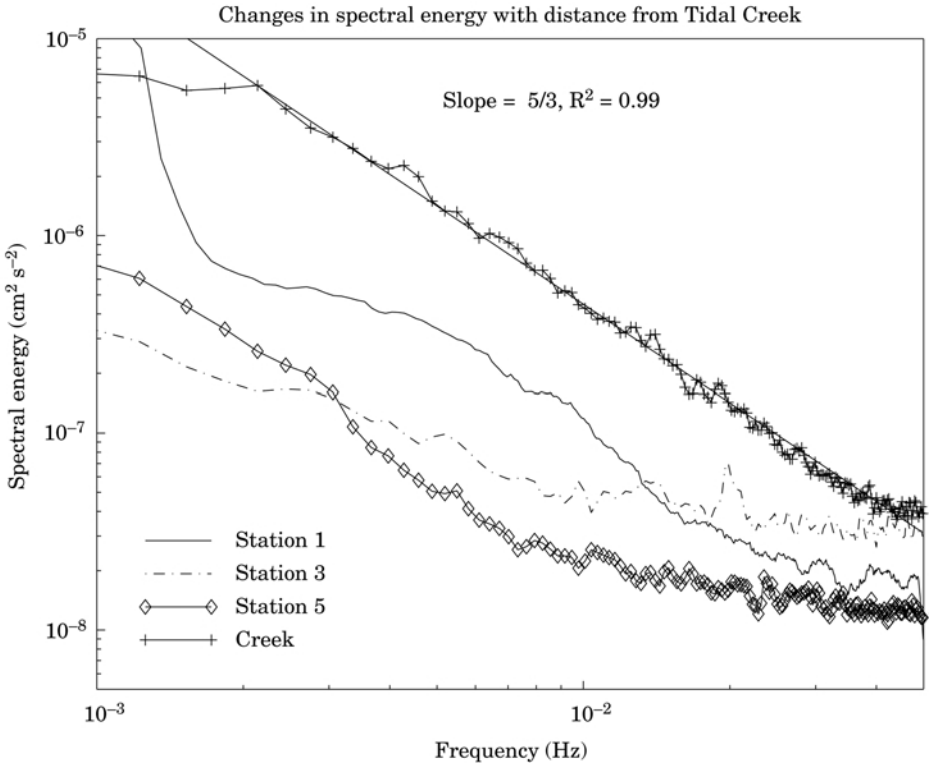


FIGURE 6. Turbulence spectra at the three sampling stations 1, 3 and 5. All spectra were calculated for a 819·2 s data segment on the rising tide and on the falling tide. The spectra are scaled such that the area under each spectrum is equivalent to the variance of the turbulent fluctuations.

of larger turbulent eddies and it is likely that the vegetation also contributes to the break down of larger eddies into smaller ones. Similar spectral characteristics were observed by Leonard and Luther (1995).

Turbulent energy was reduced by a factor of 5 between the tidal creek and the vegetation boundary. It continued to decrease with distance across the marsh surface as the flow progressed into the vegetation canopy [Figure 7(a)]. Turbulent energy levels at the creek bank stations reflected the conditions in the tidal creek on the rising tide; the energy levels were higher and follow the changes seen in the creek. On the falling tide flow velocities increased but the increase was not matched by production of turbulent energy. At this time, the flow was from the marsh interior to the creek, and the turbulent energy reflected conditions within the canopy, characterized by lower turbulent energy levels. There was no correlation between turbulent energy levels in the canopy and turbulent energy in the tidal creek on the falling tide [Figure 7(a)].

Reynolds number within the vegetation canopy ranged from 250–500 (indicating laminar flow), but the energy in the spectra (Figure 6) suggests that the flow was in a transitional regime where there was some production of kinetic energy, although not as much as in a fully turbulent flow. Marsh surface flows measured by Leonard and Luther (1995) were also transitional.

Shear velocities were calculated for all time series measured at stations 1 and 5 [Figure 7(b,c)]. At

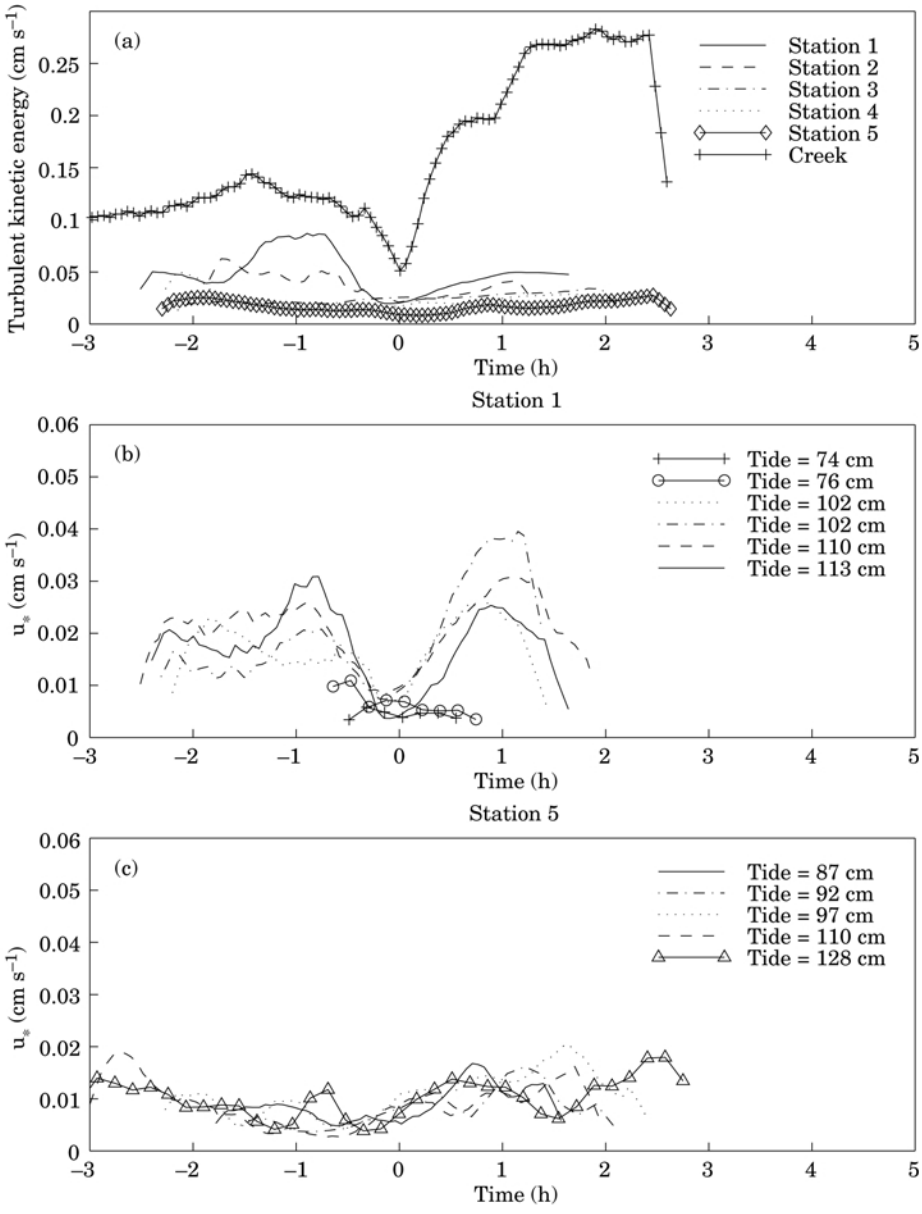


FIGURE 7. (a) Variation in turbulent kinetic energy in the tidal creek and at stations 1–5. (b) Variation in shear velocity with time at station 1 at a range of tidal amplitudes. (c) Variation in shear velocity with time at station 5 at a range of tidal amplitudes. The shear velocity at station 1 is representative of conditions on the creek bank and levee, and station 5 is representative of conditions in the interior.

station 1, shear velocities remained low throughout the duration of the lowest tides (amplitudes 74 and 76 cm). During these low amplitudes, the marsh surface was only flooded for a short period of time (1 h) during slack tide. Tides with amplitudes >100 cm reflect the temporal variation in the tidal flow; higher values of shear velocity correspond to times of higher flow velocity. At station 5, in the marsh interior, a similar temporal variation in shear velocity was not observed and shear velocities at this location tended to be lower than at the marsh edge. For tides with amplitudes ranging 90–130 cm, there was little variability in maximum shear velocity among tides.

### *Sediment concentrations*

Sediment concentration on the marsh surface varied with time relative to high tide and with distance from the tidal creek (Figure 8). On the rising part of the tide, sediment concentrations were higher on the creek bank than in the marsh interior. At station 1, sediment concentrations increased on the rising tide.

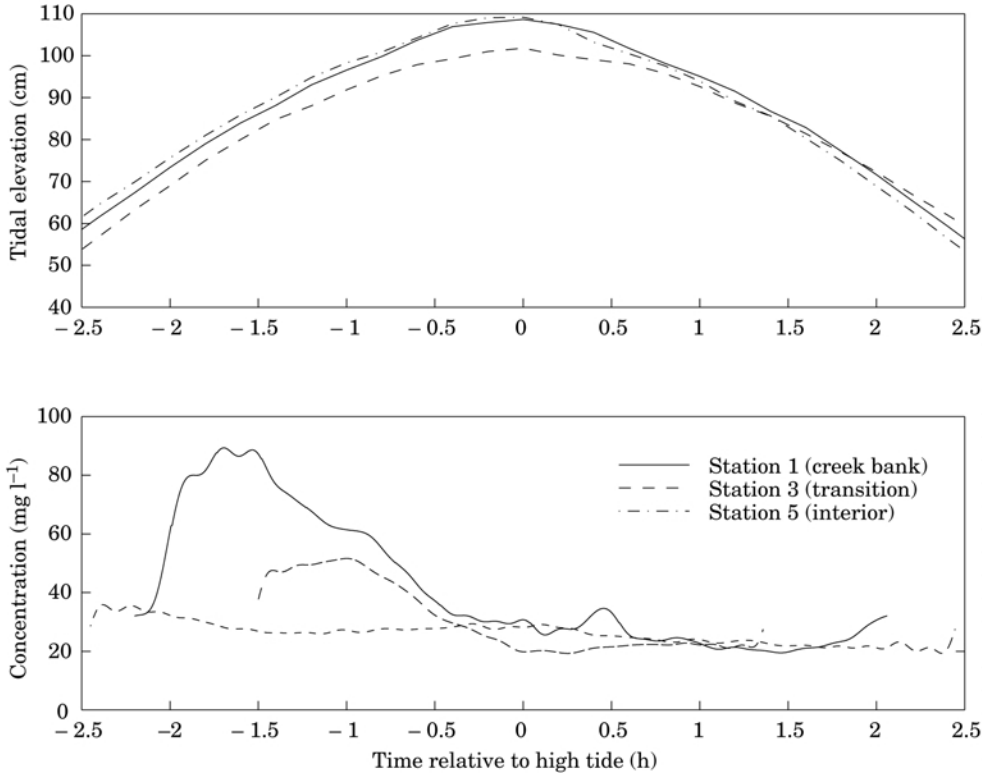


FIGURE 8. Change in sediment concentration with time and with distance from tidal creek.

As slack tide was approached, the concentration levels dropped in response to decreased sediment supply from the creek. A similar pattern was observed at station 3, the transition between creek bank and interior, although peak concentrations fell to half the values at station 1. Flow direction on the rising tide was from the creek towards the marsh interior, and consequently, the decrease in sediment concentration on the rising part of the tide indicates deposition on the creek bank. Sediment concentrations did not increase on the falling tide, despite the higher velocities and stresses on the marsh surface. This was true at all tidal amplitudes, indicating that resuspension did not occur on the marsh surface.

Sediment concentrations on the creek bank (station 1) increased in response to increased tidal amplitude whereas concentrations in the marsh interior (station 5), did not (Figure 9 and 10). The difference between the response at these two stations, in conjunction with the general direction of flow on the marsh surface, implies that a portion of sediment brought onto the marsh at station 1, was deposited in the vicinity of the creek bank rather than advected to station 5. This observation is consistent with the low mean flow velocities on the marsh surface. The large variability in sediment concentration at the creek bank as a function of tidal amplitude suggests that sediment deposition also varied strongly with tidal amplitude. At station 5, the concentrations are likely to reflect background levels of fine suspended particles with settling velocities too low to have permitted the particles to settle out of suspension over one tidal cycle.

The temporal variation in shear velocity at station 1 was compared to the temporal variation in suspended sediment concentration to determine whether concentrations decreased in response to decreased ability of the flow to maintain sediment in suspension (Figure 11). This comparison showed that the decrease in sediment concentration occurred 40–60 min earlier, relative to high tide, than the decrease in shear velocity. From this it can be concluded that even the highest shear velocities within the canopy were inadequate to maintain the largest particles in suspension. It is, however, likely that the turbulence was sufficiently strong to reduce the rate of particle deposition.

Estimated values of $u_\star$ at station 1 (Figure 7) indicate that on the rising tide, the highest value of $u_\star$ was 0·03 cm s$^{-1}$. Based on the Rouse number criterion for full suspension ($P_m$<0·3), the turbulence of the flow can maintain flocculated particles with diameters less than 50 μm in suspension (using Equation 3 to calculate $w_s$), or individual particles with diameters less than 10 μm (using Equation 2 to calculate $w_s$) (Table 2).

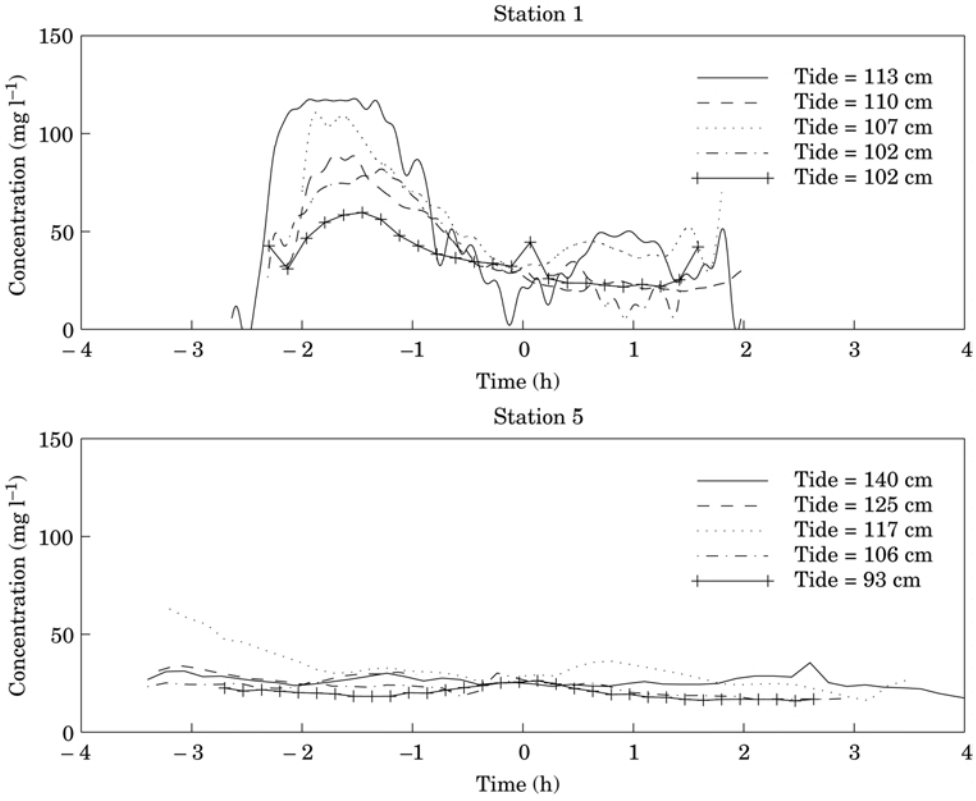


FIGURE 9. Sediment concentration as a function of time at station 1 and station 5. The measurements were made at tides of different amplitude. At station 1, on the creek bank, sediment concentrations respond to changing amplitudes, whereas in the marsh interior (at station 5) they do not. Although the concentration levels vary among tides at station 1, the temporal pattern is consistent between tides.

*Grain size distributions*

Grain size distributions of sediment from stations 1–4 are shown in Figure 12. Particle sizes range from 0·7 μm to 64 μm. The lower size limit (0·7 μm) is the operational limit of the Coulter Multisizer. The small value of the modal size along with a small value of maximum diameter indicates that particles were derived from a low energy environment. The measured grain size distributions of particles deposited at stations 1–3 are very similar [Figure 12(a)], whereas the grain size distribution of sediment deposited at station 4 is finer.

Following the approach of Milligan and Loring (1997), the coefficients $\Delta Q$ and $\bar{k}$ in Equation 1 were found by fitting Equation 1 to the coarse and the fine end of the grain size distributions in a least squares sense. The floc settled part of the distribution is indicated by the dash-dotted line and the single-grain settled part is indicated by the dashed line in Figure 12(b–e); the coefficients resulting from these fits are given in Table 3. The sum of the two curves (calculated distribution) is indicated by the solid lines in Figure 12. At stations 1–3 the agreement between measured and calculated distributions is good: $R^2$=0·925–0·989 (Table 3). At station 4, the coarsest particles (particles >20 μm) are not explained, but these particles represent only 10% of all particles. It is our hypothesis that these coarser particles were introduced at times not associated with normal deposition, for example by crabs moving at the site.

The floc limit and the percentage of floc settled material are given in Table 3. The floc limit decreased from 19 μm at station 1 to 3 μm at station 4, suggesting that the size of particles incorporated in flocs decreased from station 1 to station 4. In addition, the percentage of material moving as flocs decreased from approximately 75% on the creek bank (station 1) to 20% in the marsh interior (station 4). At stations 1–3, the single grain settled portion of the curve is less prominent than at station 4 [Figure 12(b–e)], suggesting that most of the flocculated material did not reach the marsh interior. The single grains that settled out at station 4 are likely to have been small particles not incorporated into flocs. The relatively small difference between the amount of sediment in the mode and in the fine tail of the distributions in Figure 12(b–e)

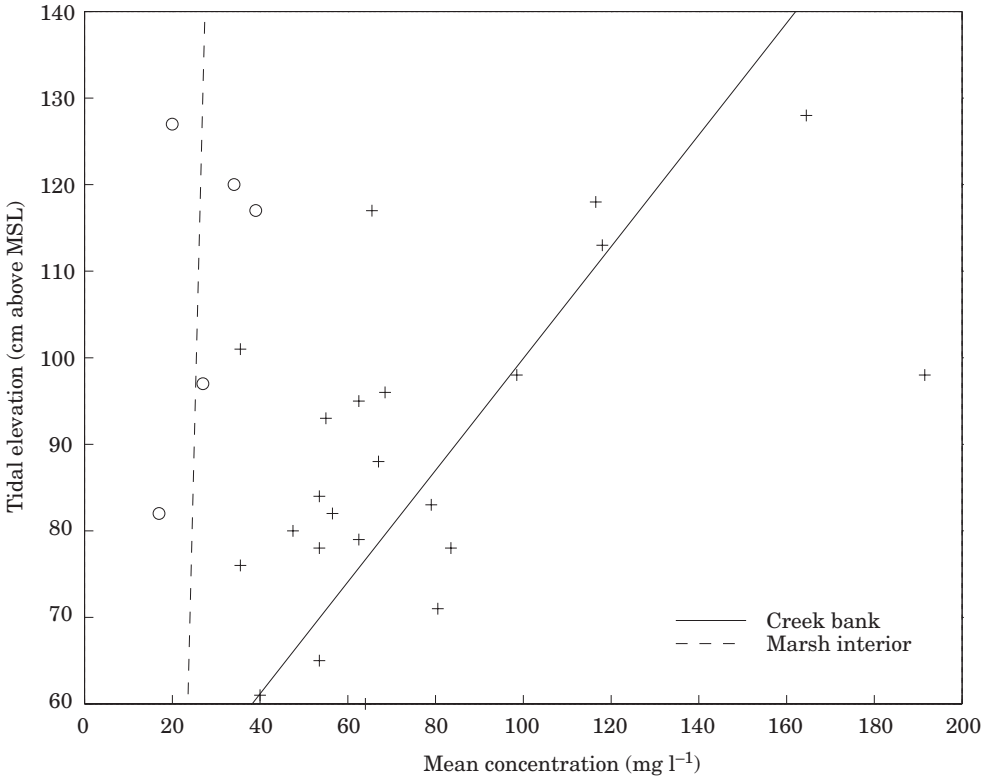


FIGURE 10. Concentration as a function of tidal amplitude on the creek bank and in the interior. On the creek bank, the regression line between measured concentrations and tidal elevation has an $R^2$=0·48, $P$=0·001. In the interior, there is no correlation between measured concentration and water level ($R^2$=0·01, $P$=0·36).

suggests that flocculated material deposited at all locations, although a higher proportion sediment deposited at stations 1–3 was flocculated (70–80%) than at station 4 (20%). The predominance of floc settled material and absence of coarser, well sorted material is a strong indication that resuspension did not occur after initial deposition (Kranck *et al.*, 1996*a*).

## Discussion

### *Controls on mean flow velocity and direction*

Mean flow speed and direction in Phillips Creek were controlled by tidal forcing. Flow speed decreased as the highest water level was approached and increased again on the falling tide. Once tidal levels in the creek exceeded creek bank elevation, a similar pattern in mean flow speed and direction was observed at station 1, although flow direction at this location was perpendicular to the flow in the tidal creek (Figure 5). A tidal influence on flow direction was observed at all five stations along the transect, with water flowing from Phillips Creek towards the interior on the rising tide and reversing on the falling tide. A more pronounced difference in flow speed between rising tide, slack water and falling tide was observed on the creek bank than in the marsh interior. In the interior, mean flow appeared more strongly modified by vegetation. All flow speeds measured on the marsh were extremely low (<1 cm s$^{-1}$). Velocities were lower in the marsh interior than on the creek bank but no measured velocities exceeded 1 cm s$^{-1}$. Tides with higher amplitudes did not produce higher flow velocities at any station on any of the tides observed in this study (Figure 4).

Mean flow velocities observed on Phillips Creek marsh are significantly lower than mean velocities measured on marsh surfaces by Leonard and Luther (1995) (5–10 cm s$^{-1}$) and Burke and Stoltzenbach (1983) (5 cm s$^{-1}$). Although the mean flow velocity was lower within the vegetation canopy than it would have been at the same location if there was no vegetation, its order of magnitude was determined by regional scale forcing of the flow. In this case, regional scale refers to the area around the entire length of Phillips Creek [Figure 1(b)]. Mean flow speed is controlled by water surface slope, which in turn depends on the spatial gradient of the tidal wave, vegetation roughness of the marsh surface, and the landscape topography in the Phillips Creek area. It

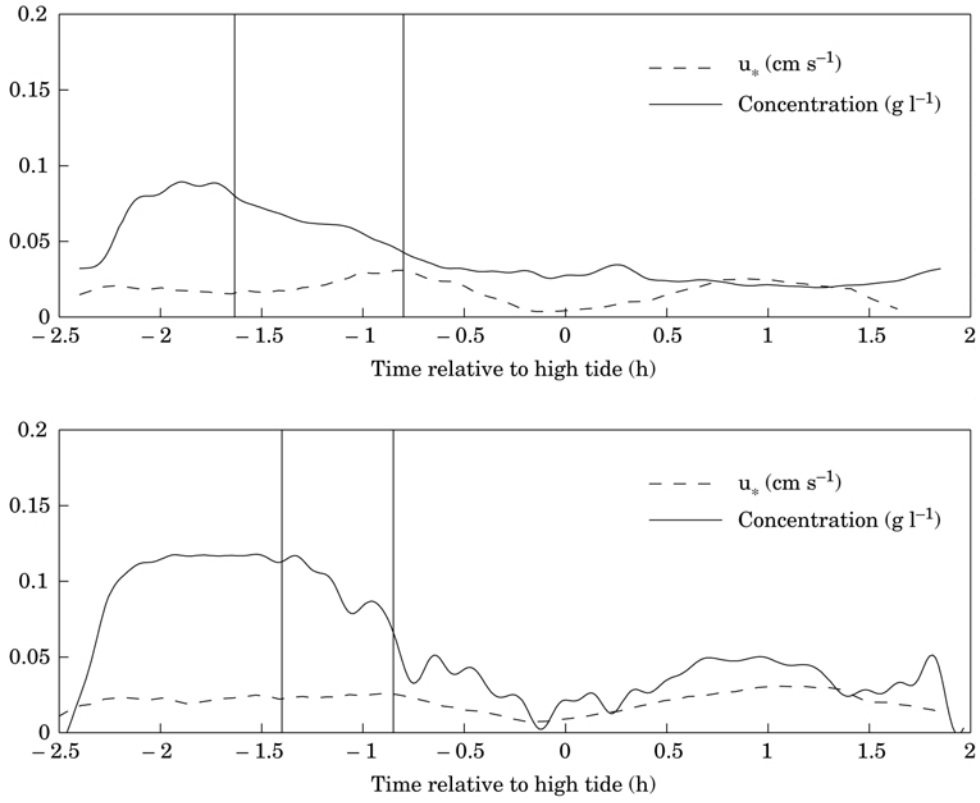


FIGURE 11. Comparison between temporal variation in concentration and shear velocity for two different tides. The vertical lines indicate onset of decreasing sediment concentration and onset of decreasing shear velocity. In the top panel, tidal amplitude was 110 cm, in the bottom panel tidal amplitude was 113 cm. Both sets of measurements were made at station 1.

TABLE 2. Estimate of particle sizes maintained at the indicated Rouse number: $P_m = w_s/u_\star$. When $P_m > 1$, sediment cannot be maintained in suspension, and when $P_m < 0{\cdot}3$, sediment is maintained in suspension

| Location | $u_\star$ (cm s$^{-1}$) | $P_m$ | $w_s$ (cm s$^{-1}$) | $D_m$ (Stokes law, Eqn 2) μm | $D_m$ (Flocs, Eqn 3) μm |
|---|---|---|---|---|---|
| Creek bank | 0·03 | 0·3 | 0·009 | 10 | 50 |
| Marsh interior | 0·01 | 0·3 | 0·003 | 6 | — |
| Creek bank | 0·03 | 1 | 0·03 | 18 | 115 |

is characteristic of the Phillips Creek area that the landscape slopes downward in the seaward direction; the marshes further landward are at a slightly higher elevation than the study site. As water level in the area increases, the wetted surface area of the marsh gradually increases, causing divergence of the flow. At the study site, flow velocities were estimated using marsh surface topography and water elevation change over a tidal cycle. The velocities estimated in this manner (0·5–1·5 cm s$^{-1}$) were in relatively good agreement with measured velocities.

Velocities measured at all stations on the marsh surface (Figure 5) indicated higher velocities on the falling tide than on the rising tide. The seaward landscape slope may in part explain this asymmetry observed between velocities on the flood and ebb tide. In addition, resistance to the flow increased in the on-marsh direction, an effect that would also act to decrease velocities of flow onto the marsh and increase flow velocities leaving the marsh.

### *Turbulence and sediment transport*

Vegetation on the marsh surface modified the hydrodynamical environment to one that favoured sediment deposition. Measurements of $u_\star$ within the canopy

TABLE 3. Diameter of mode, regression coefficients, floc limit and percentage of material deposited from a flocculated source, derived from particle size distributions of sediment deposited at stations 1, 2, 3 and 4

| | Station 1 | Station 2 | Station 3 | Station 4 |
|---|---|---|---|---|
| Mode (μm) | 15 | 18 | 19 | 11 |
| Coarse fraction | | | | |
| $\Delta Q$ | 293 | 370 | 353 | 1980 |
| $\bar{k}$ | 18·2 | 18·6 | 19·3 | 105 |
| $m+n$ | 1·2 | 1·2 | 1·2 | 1 |
| Fine tail | | | | |
| $\Delta Q$ | 12·7 | 12·0 | 11·8 | 2·2 |
| $\bar{k}$ | 34 | 39 | 28 | 674 |
| $m+n$ | 0·2 | 0·2 | 0·2 | 0 |
| $R^2$ | 0·925 | 0·940 | 0·989 | 0·74 |
| Floc limit (μm) | 19 | 17 | 19 | 3 |
| % flocs | 77 | 69 | 74 | 20 |

indicate that the shear velocity of the flow decreased with distance from the tidal creek; the most dramatic decrease was observed at the vegetation boundary, in the transition between tidal creek and marsh (Figure 7, top panel). On the marsh surface, the greatest reduction in turbulent energy occurred across the creek bank. At station 3, 8 m from the tidal creek, the turbulent structure was similar to the structure at station 4, 27 m from the creek and station 5, 46 m from the creek (Figure 7).

Particle size distributions support a decreased transport capacity between stations 1–3 on the creek bank and station 4 in the interior. The relative proportion of particles greater than 15 μm was reduced between these locations [Figure 12(a)], which was also the particle size that approximately corresponds to the floc limit at the creek bank stations (Table 3). Particles with diameters greater than 15 μm settled as single particles whereas the smaller particles predominantly settled as flocs. The lack of correspondence between the timing of the decrease in shear velocity and sediment concentration on the creek bank (Figure 11) suggests that the flocs settling out of suspension are larger than 50 μm (based on the Rouse number criterion of 0·3 and Equation 3). The settling velocities of these flocs, combined with low advection velocities, result in deposition in proximity to the tidal creek. This is consistent with the analysis of the size distributions indicating that 70–80% of the sediment on the creek banks settled as flocs.

In the marsh interior, the flow can only maintain individual particles with diameters less than 6 μm in suspension (Table 2). The floc limit at station 4 (3 μm) was smaller than at stations 1–3, indicating that smaller particles comprised each floc, and possibly that flocs deposited at this location were smaller than the flocs deposited at the creek bank stations. At station 4, only 20% of the material deposited was derived from a flocculated source (Table 3). The smaller floc limit at station 4 suggests that larger flocs are deposited before reaching station 4.

Concentration levels measured simultaneously in the creek, at station 1 and at station 2, indicate that concentrations on the marsh surface near the creek bank were directly correlated with sediment concentrations in the creek, and that concentrations in flows over the marsh surface declined in response to decreased concentration in the creek. This observation implies that processes in the tidal creek are controlling the amount of sediment settling on the marsh surface rather than processes on the marsh surface itself. Sediment concentrations on the creek bank and levee were consistently higher on the rising tide than on the falling tide, indicating that deposition occurred on the rising tide. Sediment concentrations decreased significantly between station 1 and station 3, indicating deposition in vicinity of the tidal creek.

There was no indication of resuspension of sediment from the marsh surface at any time including falling tide when velocities and stresses on the marsh surface were greatest. The maximum boundary shear stress along the marsh transect was measured on the levee: $\tau_b = 0{\cdot}001$ dy cm$^{-2}$. In comparison, Widdows *et al.* (1998) determined critical erosion stresses ranging from 1·7 dy cm$^{-2}$ to 7 dy cm$^{-2}$ for estuarine mud in the U.K. The critical erosion stress for Phillips Creek marsh sediments is likely to be different from that of the U.K. estuarine mud, but its precise value is unknown. Comparing $\tau_b$ to the lower end of this range of critical erosion stresses, however, yields a 3 order of magnitude difference. A critical erosion stress of this

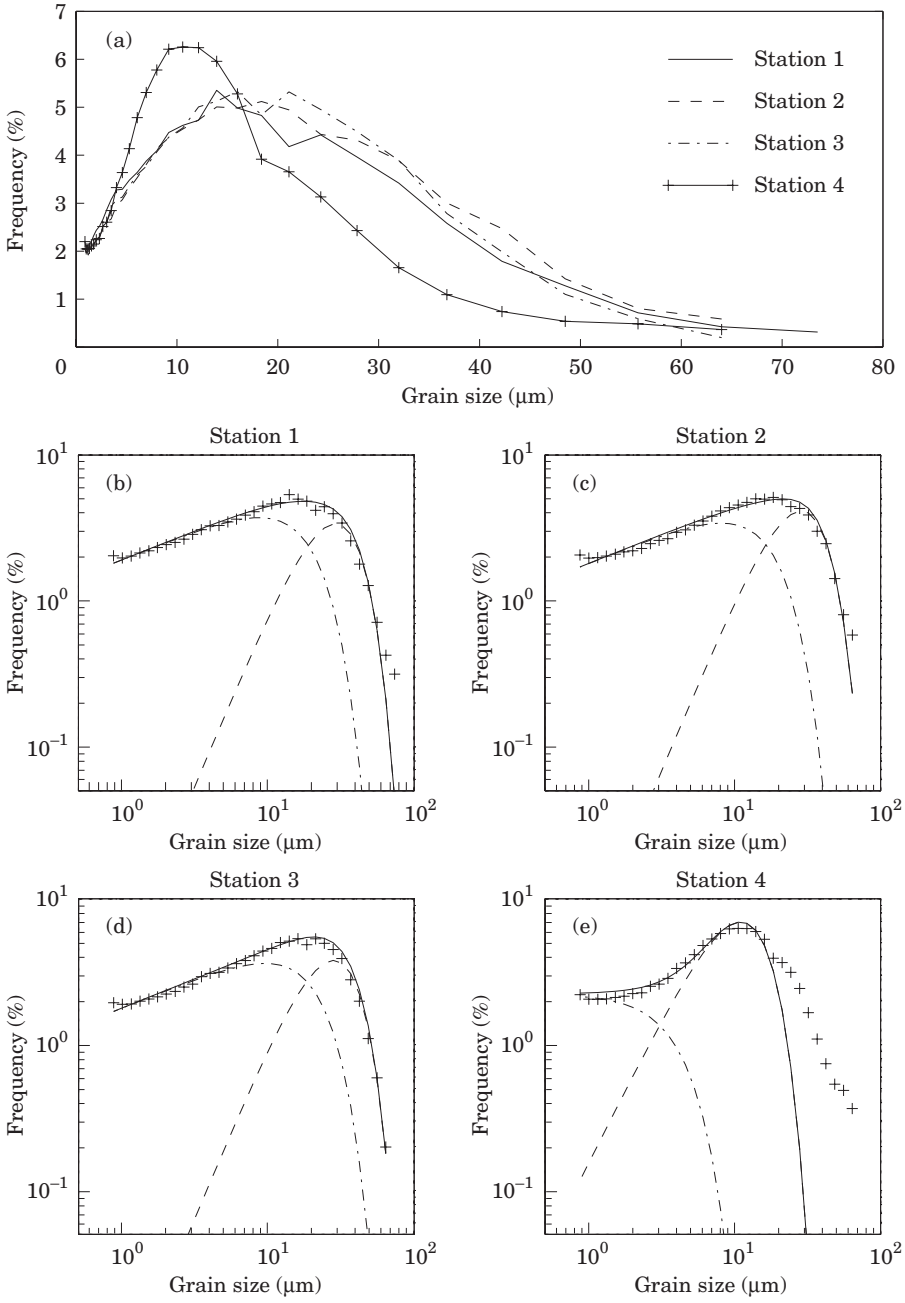


FIGURE 12. Particle size distributions of fully disaggregated sediment. (a) Comparison of measured particle size distributions for fully disaggregated sediment. (b–e) Measured particle size distributions on a log–log scale (marked '+'). Curves describing the floc settled portion of the sediment are indicated by the dash-dotted line and curves describing the single grain portion of the curve is marked by the dashed lines. The sum of the two curves is marked by the solid line. The curves have been obtained by fitting Equation 1 respectively to the coarse and the fine end of the measured distributions. Coefficients from the fits are listed in Table 3.

magnitude is not likely to have been exceeded during any of the flow conditions measured on Phillips Creek marsh. In addition, grain size distributions support the absence of sediment resuspension after initial deposition.

## Conclusions

Sediment deposition on Phillips Creek marsh occurred owing to the combined effects of flocculation of fine sediment in the water column, which allowed

particles to settle at higher rates than they would have individually, and reduction of turbulence levels within the vegetation canopy. Flow velocities on the marsh surface were low ($<1$ cm s$^{-1}$) during all tidal conditions measured. The combination of low flow velocities and relatively high settling rates of most flocs and single grains promoted deposition in vicinity of the tidal creek. Disaggregated inorganic grain size distributions of the sediment on the marsh surface indicate that 70–80% of the sediment deposited within 8 m of the tidal creek was in a flocculated form. In the marsh interior, 25 m from the tidal creek, only small individual grains and small flocs were deposited.

Sediment was deposited on the marsh surface at tidal elevations ranging from tides barely overtopping the creek bank to high spring tides. During all tidal conditions, suspended sediment concentrations at the marsh edge were higher on the rising tide than on the falling tide. Sediment concentrations along the sampling transect decreased with distance from the tidal creek. Combined with tidal flows across the creek bank that were oriented perpendicular to the tidal creek, these patterns indicate sediment deposition on the marsh surface during flood tides. Suspended sediment concentrations at the creek bank increased with tidal amplitude while concentrations in the marsh interior did not. Therefore, while the processes controlling sediment deposition did not vary among tides, more sediment was brought into the marsh during higher tides, promoting higher rates of deposition.

Measured shear stresses within the *S. alterniflora* canopy were insufficient to remobilize sediment from the marsh surface after initial deposition and increases in sediment concentration resulting from sediment resuspension during peak ebb-tide flows were not observed. This is consistent with the analysis of the disaggregated grain size distributions which indicated that sediment deposited on the marsh surface was not resuspended after initial deposition.

## Acknowledgements

This research was sponsored by and conducted as part of the Virginia Coast Reserve—Long Term Ecological Research site. Dr John Porter, Jimmy Spitler, and David L. Richardson of the VCR-LTER made data available and were a tremendous help in the field. Our warm thanks to Dr Carl Friedrichs, Frank Farmer and Todd Nelson at the Physical Oceanography Department at Virginia Institute of Marine Science for providing facilities to calibrate the OBS sensors and for helping with wiring and programming of the ADV, and to Dr Morten Pejrup at the University of Copenhagen for hosting the first author in the writing phase of this manuscript.

## References

Burke, R. & Stoltzenbach, K. 1983 *Free Surface Flow Through Salt Marsh Grass*. MIT Sea Grant College Program.

Cahoon, D., Reed, D. & Day, J. J. W. 1995 Estimating shallow subsidence in microtidal salt marshes of the southeastern United States: Kaye and Barghoorn revisited. *Marine Geology* **128,** 1–9.

Emery, K. & Aubrey, D. 1991 *Sea Levels, Land Levels and Tide Gauges*. Springer-Verlag, Berlin.

French, J., Spencer, T., Murray, A. & Arnold, N. 1995 Geostatistical analysis of sediment deposition in two small tidal wetlands, Norfolk, U.K. *Journal of Coastal Research* **11,** 308–321.

Holdahl, S. & Morrison, N. 1974 Using precise relevelings and mareograph data. *Tectonophysics* **23,** 373–390.

Kadlec, R. 1990 Overland flow in wetlands: vegetation resistance. *Journal of Hydraulic Engineering* **116,** 691–706.

Kastler, J. 1973 *Sedimentation and Landscape Evolution of Virginia Salt Marshes*. Master's thesis, University of Virginia.

Kastler, J. & Wiberg, P. 1996 Sedimentation and boundary changes of Virginia salt marshes. *Estuarine, Coastal and Shelf Science* **42,** 683–700.

Kranck, K., Smith, P. & Milligan, T. 1996*a* Grain-size characteristics of fine grained unflocculated sediments I: 'one-round' distributions. *Sedimentology* **43,** 589–596.

Kranck, K., Smith, P. & Milligan, T. 1996*b* Grain-size characteristics of fine grained unflocculated sediments II: 'multi-round' distributions. *Sedimentology* **43,** 597–606.

Leonard, L. 1997 Controls of sediment and deposition in an incised mainland marsh basin, Southeastern North Carolina. *Wetlands* **17,** 263–274.

Leonard, L. & Luther, M. 1995 Flow hydrodynamics in tidal marsh canopies. *Limnology and Oceanography* **40,** 1474–1484.

Milligan, T. & Kranck, K. 1991 Electroresistance particle size analyzers. In *Principles, Methods, and Application of Particle Size Analysis* (Syvitski, J., ed.). Cambridge University Press, Cambridge, pp. 109–118.

Milligan, T. & Loring, D. 1997 The effect of size distributions of bottom sediment in coastal inlets: implications for contaminant transport. *Water, Air and Soil Pollution* **99,** 33–42.

Nerem, R., van Dam, T. & Schenewerk, M. 1998 Chesapeake Bay subsidence monitored as wetland loss continues. *EOS* **79,** 156–157.

Peltier, W. & Jiang, X. 1996 Mantle viscosity from the simultaneous inversion of multiple data sets pertaining to post-glacial rebound. *Geophysical Research Letters* **101,** 503–506.

Robinson, S. 1994 *Clay Mineralogy and Sediment Texture of Environments in a Barrier Island-lagoon System*. Master's thesis, University of Virginia.

Sternberg, R., Berhane, I. & Ogston, A. 1999 Measurement of size and settling velocity of suspended aggregates on the Northern California continental shelf. *Marine Geology* **154,** 43–53.

Stevenson, J., Kearney, M. & Pendleton, E. 1985 Sedimentation and erosion in a Chesapeake Bay brackish marsh system. *Marine Geology* **67,** 213–235.

Tennekes, H. & Lumley, J. 1972 *A First Course in Turbulence*. The MIT Press.

Tsujimoto, T., Kitamura, T. & Okada, T. 1991 Turbulent structure of flow over rigid vegetation covered bed in open channels. In *KHL Progressive Report*, Hydraulics Laboratory, Kanazawa University, pp. 1–14.

Wang, F., Lu, T. & Sikora, W. 1993 Intertidal marsh suspended sediment transport processes, Terrebonne Bay, Louisiana, USA. *Journal of Coastal Research* **9,** 209–220.

Wiberg, P., Drake, D. & Cacchione, D. 1994 Sediment resuspension and bed armoring during high bottom stress events on the northern California inner continental shelf: measurements and predictions. *Continental Shelf Research* **14,** 1191–1219.

Widdows, J., Brinsley, M., Bowley, N. & Barret, C. 1998 A benthic annular flume for *in situ* measurement of suspension feeding/biodeposition rates and erosion potential of intertidal cohesive sediments. *Estuarine, Coastal and Shelf Science* **46,** 27–38.